



Influence of contact resistance on shielding efficiency of shielding gutters for high-voltage cables

S. Koroglu¹ P. Sergeant^{2,*} R.V. Sabariego³ V.Q. Dang³ M. De Wulf⁴

¹Faculty of Engineering, Department of Electrical and Electronics Engineering, Pamukkale University, 20070 Denizli, Turkey

²Department of Electrical Energy, Systems and Automation, Ghent University, B-9000 Ghent, Belgium

³ACE, Department of Electrical Engineering and Computer Science, University of Liège, B-4000 Liège, Belgium

⁴ArcelorMittal Global R&D Gent, B-9060 Zelzate, Belgium

*Department of Electrotechnology, Faculty of Applied Engineering Sciences, University College Ghent, B-9000 Ghent, Belgium

E-mail: skoroglu@pau.edu.tr; slm.koroglu@gmail.com

Abstract: The shielding of buried three-phase high-voltage power lines can be done by placing them in conducting ferromagnetic U-shaped gutters covered with plates. In case of a perfect electrical contact between adjacent gutters and between adjacent cover plates, induced currents in the shield efficiently reduce the magnetic field generated by the cables. As however a perfect contact cannot be guaranteed, in practice, it is useful to quantify the effect of a defective electrical contact on the field reduction. From two-dimensional/three-dimensional finite element computations and experiments, the influence of the contact resistance on the shielding efficiency is investigated, as a function of the ratio of axial length to height of the shield elements. Furthermore, the effect of other parameters on the shielding efficiency is studied: the ratio of axial length to height, a parasitic air gap between the gutter and the cover plate and the type of the shield material. It was found that a low contact resistance deteriorates much more the shielding in case of an aluminium shield than in case of a steel shield. As expected, the effect is larger for shield elements with relatively short axial length with regard to the other dimensions. Nevertheless, the effect remains quite significant for aluminium shields with practically convenient dimensions.

1 Introduction

Many disturbing magnetic sources exist in real world and in particular in electric power applications such as induction heating systems, electrical motors, high-power equipments, power transmission lines, substations and industrial transformer [1–4]. The low-frequency magnetic field produced by buried high-voltage (HV) power lines has drawn a great attention in recent years. The magnetic induction in the vicinity of these cables can reach levels of a few μT or more, depending on the distance from them, the currents they carry and the cable configuration [5]. These field levels are undesirable, as they may produce electromagnetic interferences in electric and electronic equipment and cause health hazards.

In [6–8], the magnetic shielding of extremely low-frequency HV cables is studied. According to [6], open shield configurations (e.g. flat sheets above buried cables) can provide good shielding performance if they are sufficiently large and thick. It is, however, shown in [7] that a bad contact between adjacent shielding sheets strongly deteriorates the performance of the shield. In [8], perfectly closed and open shield configurations are investigated. The shielding efficiency of the former proves to be much higher. It is thus interesting to study the effect of the contact

resistance R_c on the performance of a closed shield configuration. Let us consider a U-shaped gutter covered with a flat plate (see Fig. 1 and Table 1).

We tackle the problem with three different approaches, further explained in Section 2:

- a two-dimensional (2D) finite element model (FEM) in the xy -plane (Fig. 1);
- a full 3D FEM that accurately accounts for the overlapping zones and thus the contact resistance R_c [9];
- measurements on an experimental set-up.

The U-shaped gutter elements, used to shield the three-phase HV cables, are slightly conical in the axial direction in order to stack adjacent pieces with a small overlap and improve the electric contact; see Fig. 1b. This contact ensures an optimal distribution of the induced currents in the whole structure and therefore a good shielding. In practice, the gutters are usually connected with clips to further reduce the contact resistance, without any welding. Moreover, the cover plates are stacked with a certain overlap, what does not guarantee good contact during the lifetime of the power line.

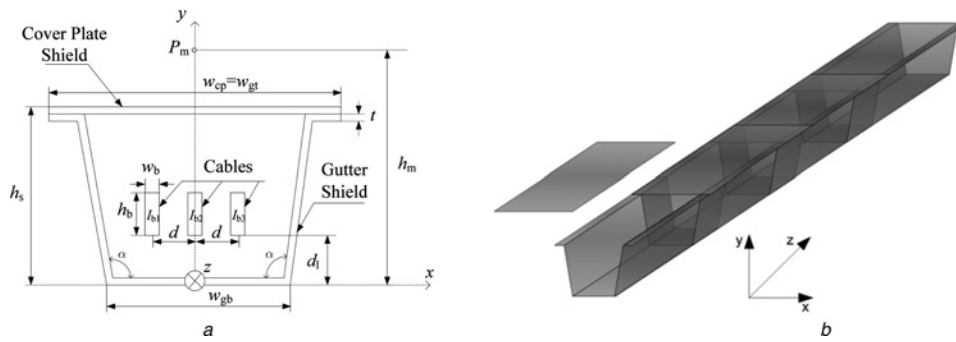


Fig. 1 Effect of the contact resistance R_c on the performance of a closed shield configuration
 a Transversal cut (xy -plane) of the buried HV cables inside the shield (gutter and CP). Dimensions are given in Table 1
 b Three-dimensional view showing the overlap between shield elements

Table 1 Dimensions of the shielding configuration

Quantity	Symbol	Experiment
width of cover plate	w_{cp}	0.520 m
width of top of gutter shield	w_{gt}	0.520 m
thickness of shield	t	0.003 m
height of shield	h_s	0.271 m
section width of bus-bars	w_b	0.005 m
section height of bus-bars	h_b	0.050 m
distance between bus-bars	d	0.10 m
distance of bus-bars from gutter bottom	d_l	0.10 m
angle of gutter shield	α	98°
width of bottom of gutter shield	w_{gb}	0.325 m

2 Numerical models

2.1 Two-dimensional FEM

We consider a time-harmonic 2D FEM based on the classical magnetic vector potential formulation, where the unknown is its z -component $A = A_z \mathbf{1}_z$.

For a shield in steel, the model uses a non-linear constitutive law obtained from hysteresis loop measurements on strips of the steel shielding material DX52 an Epstein frame. Loops were measured at 0.5 Hz and the single-valued characteristic was found from the peak values of H and B . Fig. 2 shows the characteristic curve of the magnetic permeability $\mu(B)$ and one of the measured hysteresis loops in the BH -plane. The electrical conductivity σ is the constant and equal to 6.48 MS/m. The value is obtained from a four-point measurement on a rectangular sample of the material. For a shield in aluminium, the constitutive law is linear, $B = \mu H$, with relative magnetic permeability $\mu_r = 1$ and electrical conductivity of $\sigma = 36$ MS/m.

2.2 Three-dimensional FEM

To solve the 3D magneto-dynamic problem, we consider an eddy-current problem in a bounded domain $\Omega = \Omega_c \cup \Omega_c^C$ with boundary Γ and conducting and non-conducting parts Ω_c and Ω_c^C , respectively. The shield, gutters and plates, constitute Ω_c . The cables (or bus-bars) are herein modelled as non-conducting and thus part of Ω_c^C , that is, we neglect the induced currents and suppose the imposed source is not modified.

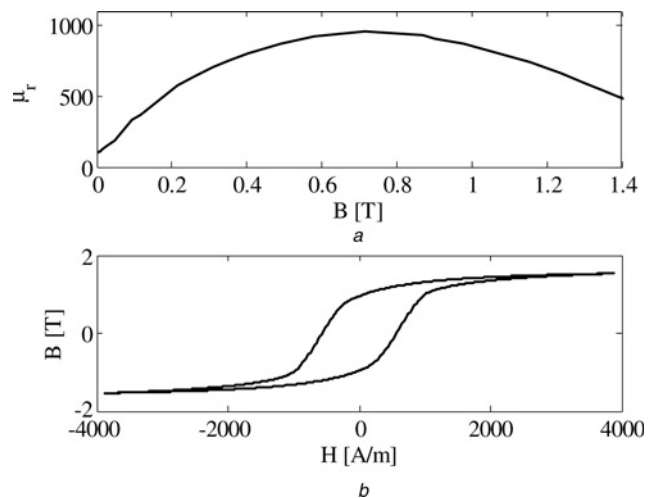


Fig. 2 Characteristic curve of the magnetic permeability
 a Relative magnetic permeability of steel DX52 against the magnetic flux density
 b Hysteresis loop in the BH -plane

As in the 2D FEM, we use a magnetic vector potential formulation, obtained from the weak form of Ampère’s law, with the electric field $\vec{E} = -\partial A$ in Ω_c and the magnetic induction $\vec{B} = \nabla \times A$ in Ω [9]. The 3D FE mesh of the studied system (see Fig. 3) comprises 229 130 hexahedra (gutter, plate and bus-bars) and tetrahedral (surrounding air), what yields to 274 063 complex unknowns. Note that for the sake of clarity, the discretisation of the air has been

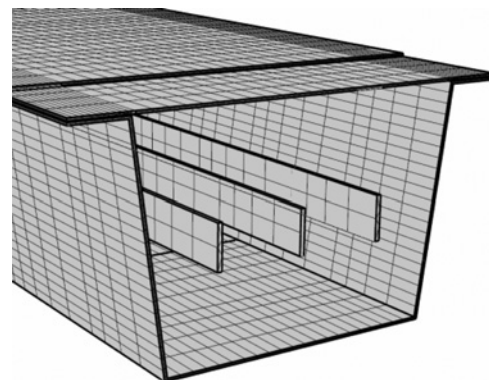


Fig. 3 Three-dimensional FEM mesh structure of the gutter with cover plate

omitted. Periodicity boundary conditions are considered. For all computations, we have taken six layers of elements along the thickness of the shield; this is enough for accounting for the eddy current variation given the working frequency and material characteristics.

3 Numerical results and discussions

In order to investigate the influence of the contact resistance effect on the shielding efficiency for HV cables, we have considered the following parameters: the ratio of axial length to height, the air gap between gutter and cover plate and the shield material.

3.1 Effect of the ratio of axial length to height

The gutters have a default ratio θ of axial length L to height H ($\theta = 1.00/0.271 = 3.69$), which is a rather large ratio. The magnetic induction distribution along the x -axis for steel shields with large ratio ($\theta = 3.69$) and with small ratio ($\theta = 2.13$) at height $y = 0.5$ m is depicted in Figs. 4a and b, respectively. The ratio of averaged induction differences in the range $x = 0, \dots, 2$ m between bad and good contact with 3D FEM results for large and small ratios are 1.13 and 1.27, respectively. We can conclude that for a shield with smaller ratio ($\theta = 2.13$), a bad contact is more critical (see Fig. 4b): the deterioration of the shielding performance is higher.

3.2 Effect of parasitic air gap between gutter and cover plate

In the ideal circumstances, the cover plate (CP) touches the gutter along the whole length of the shield. To achieve this in practice, the gutter and CP are pressed together by adding clips at regular distances along the line. However, after being buried for many years, it cannot be guaranteed that the CP still touches the gutter along the whole length of the shield. Small deformations in the soil may cause a shift or a deformation of the shielding material. In this

section, we investigate the effect of a small air gap between the gutter and the cover plate.

The magnetic flux density distribution along the x -axis for the several air gaps at height $y = 0.5$ m for a steel shield is depicted in Fig. 5. As expected, the magnetic flux density increases with the air gap. These figures show that the effect of the parasitic air gap can be seen only very close to the shield. The deterioration of the shielding is quite small at 0.5 m and even smaller for x larger than 0.5 m. We can conclude that a parasitic air gap of a few millimetres does not have much effect on the shielding.

3.3 Effect of the shielding material

Fig. 6a shows the induction levels at $y = 0.5$ m along the x -axis with the gutter and covering plate made of steel DX52 and aluminium. In case of good contact and for the same thickness, the magnetic flux density with an aluminium shield is lower than with the steel shield. Moreover, the

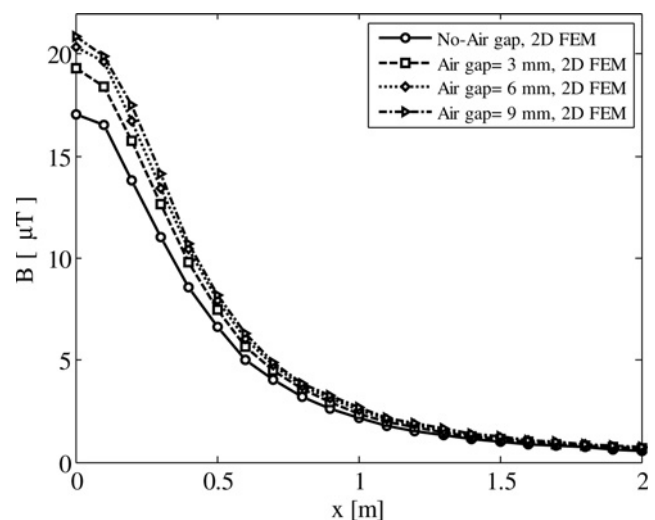


Fig. 5 Magnetic flux density against air gap between gutter and CP with steel shield at $y = 0.5$ m

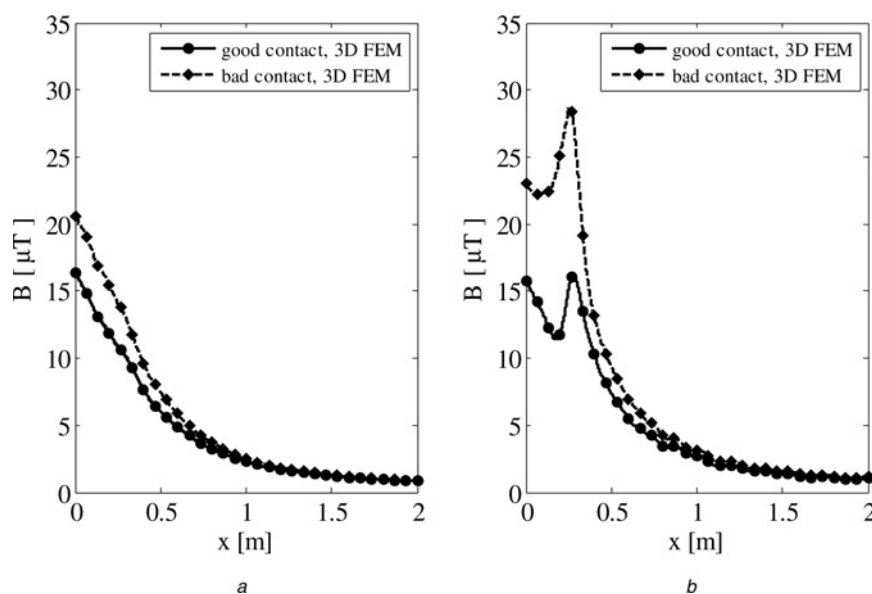


Fig. 4 Effect of bad and good contact on induction for steel shields

a With large ratio ($\theta = 3.69$)
b With small ratio ($\theta = 2.13$)

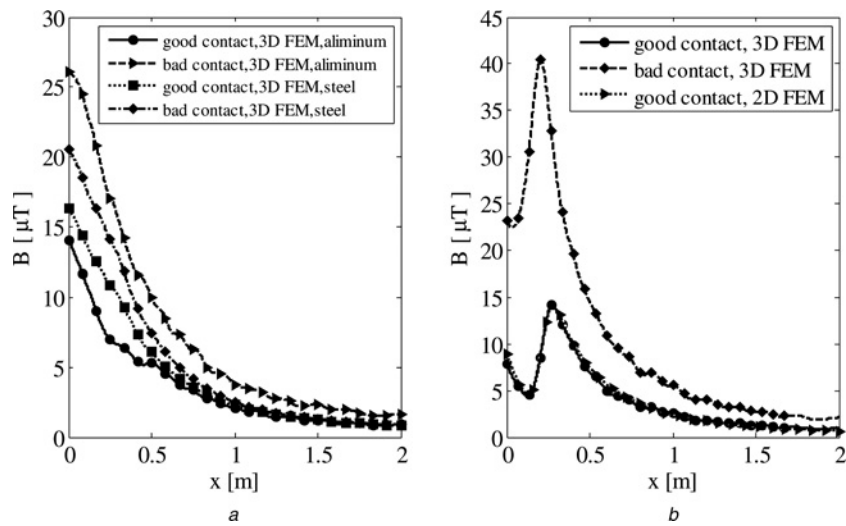


Fig. 6 Effect of good and bad contact on the magnetic flux density at $y = 0.5$ m along the x -axis
 a With the steel DX52 and aluminium shields for the default ratio $\theta = 3.69$
 b With aluminium shield for a small ratio $\theta = 2.13$

quality of the contact affects more the shielding: the ratio of average induction between bad and good electrical contact is 1.7 with aluminium and 1.3 with steel. In case of bad contact, the aluminium performs worse than the steel.

The effect of bad and good contact with aluminium shields and a small ratio ($\theta = 2.13$) is illustrated in Fig. 6b, which depicts the flux density along the x -axis at $y = 0.5$ m. The average ratio between bad and good shielding amounts to 2.50. The deterioration of the shielding performance is shown to be bigger in the aluminium shield than in the ferromagnetic shield.

Note that Fig. 6b allows also to validate the numerical models: the 2D FEM and the 3D FEM give the same results in case of good contact. Evidently, bad contact cannot be simulated by the 2D FEM.

The influence of parasitic air gaps for the aluminium shield is investigated in Fig. 7, which shows the magnetic flux density along the x -axis for several air gaps at height $y = 0.5$ m. Even a small air gap causes a quite significant deterioration of the shielding performance of the aluminium shield. Note that for aluminium the size of the gap between the CP and the gutter has virtually no effect on the shielding performance; what matters is the absence of

contact. Fig. 7 should be compared with Fig. 5, which presents the effect of the parasitic air gap in case of a steel shield. The parasitic air gap causes much more deterioration of the shielding (almost a factor 2 for an air gap of 3 mm) in case of an aluminium shield than in case of a steel shield (about 10% for an air gap of 3 mm).

In order to check the effect of the ratio θ of axial length to height on the shielding performance of shields with bad contact, 3D FEM calculations were carried out for the gutter with CP and different values of θ . Fig. 8 shows the ratio of the average induction with good contact to the average induction with bad contact for aluminium and steel. The induction is here averaged out over the region $x = 0 - 2$ m and $y = 0.5$ m. In order to vary θ , only the height of the gutter is modified without modifying any other dimension in Table 1.

One can observe that the bad contact reduces the shielding efficiency by a factor 2 for aluminium, whereas the bad contact reduces the shielding efficiency by a factor 1.17 for the steel if the axial length of a shield element is less than 3.5 times the height. For the steel shield, the bad contact has less effect, regardless of θ .

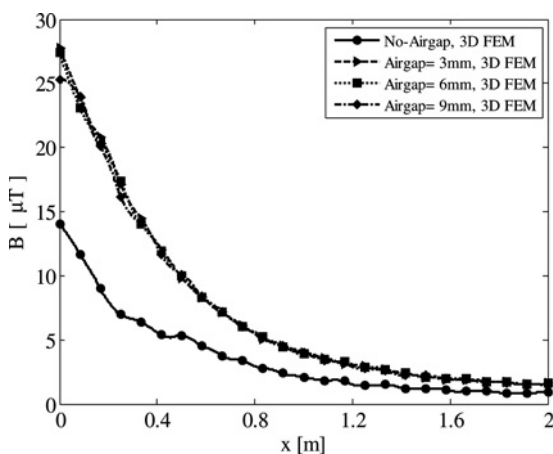


Fig. 7 Magnetic flux density against air gap between gutter and CP with aluminium shield at $y = 0.5$ m

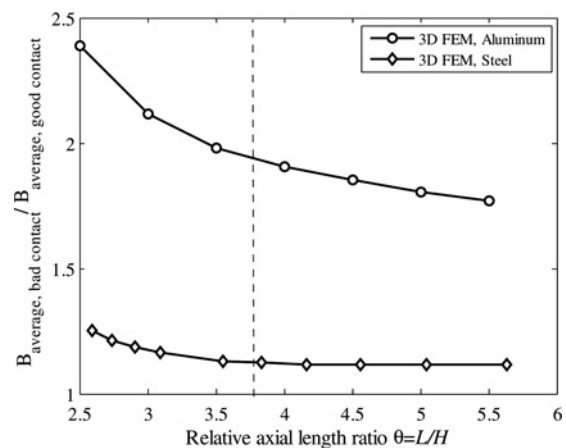


Fig. 8 Effect of bad contact on average induction for shields with different θ

Dashed line shows the default shield with $\theta = 3.69$ (dimensions in Table 1)

4 Experimental set-up and validation

In the experimental set-up, shown in Fig. 9, the three HV cables are copper bus-bars that carry adjustable balanced three-phase currents up to $I_1 = \sqrt{2} \cdot 500 \sin(\omega t + 0)$, $I_2 = \sqrt{2} \cdot 500 \sin(\omega t - 2\pi/3)$ and $I_3 = \sqrt{2} \cdot 500 \sin(\omega t + 2\pi/3)$ A (per phase current 500 A rms). The shield is 3 mm thick, made of hot rolled galvanised material (ArcelorMittal) with conductivity and induction-dependent permeability given in Section 2 and Fig. 2. The magnetic field measuring system uses a three-axial commercial field metre (accuracy $\pm 3\%$, range 0.01–200 μT and bandwidth from 30 to 2000 Hz).

In order to ensure a good electrical contact between adjacent conical U-shaped gutters, they were installed under an axial force causing high contact pressure between overlapping parts. The axial length of the overlap between sections is 200 mm. The cover plates were connected to the U-shaped gutters by clips. In order to obtain a bad contact between adjacent gutter elements, an isolating plastic foil was inserted in the overlapping zone.

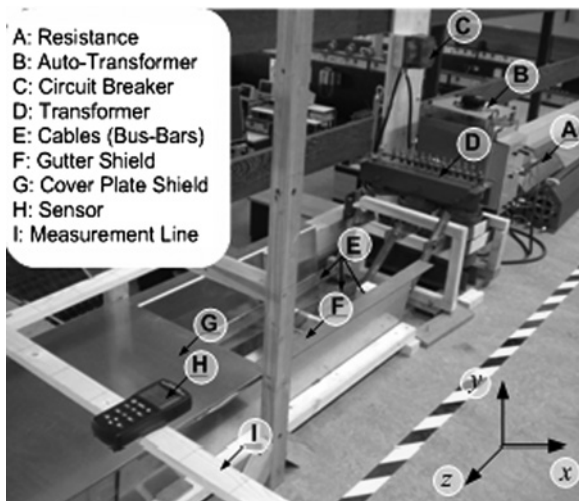


Fig. 9 Experimental set-up and xyz-reference frame at the middle of the bottom of the gutter

The effect of the contact resistance was experimentally determined for the default geometry. The measured and simulated results in the xy -plane at height $y = 1$ m are depicted in Fig. 10. One can observe that the magnetic flux density (induction) is reduced in average by a factor 2.5, when using only the gutter and by a factor 6 when using the combination gutter and CP.

In Fig. 11a, the magnetic flux density measured along the z -axis is compared with the 3D FEM results. The induction presents clear dips in the regions where two shield sections overlap.

The computed and measured magnetic flux density results, distributed along the x -axis at $y = 0.5$ m, are shown in Fig. 11b. The average ratio of the magnetic induction between bad and good contact is 1.11 and 1.13 with measurements and 3D FEM, respectively. These results validate the computations with the 3D FEM.

According to Fig. 11, the difference between the measured flux density with good contact (overlap and clips) and bad contact (plastic foil between adjacent gutters) is rather small. These results seem to contradict with those reported in [7], where the difference between good and bad contact

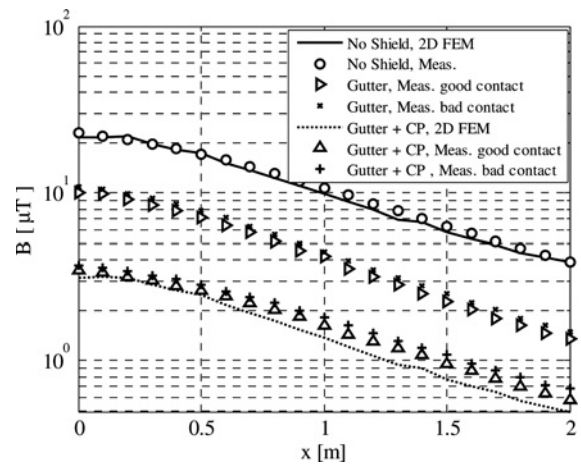


Fig. 10 Magnetic flux density at $y = 1$ m for several shield configurations for a phase current of 500 A rms

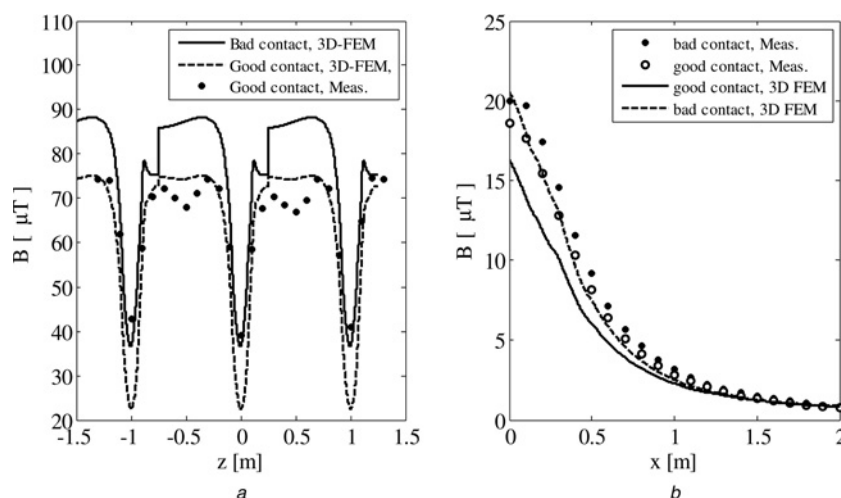


Fig. 11 Computed and measured magnetic flux density with the gutter and CP made of steel

a At $x = 0$ m and $y = 0.28$ m along the z -axis
 b At $y = 0.5$ m and $z = 0$ m along the x -axis

when using cover plates is always significant. However, this is justified when comparing the dimensions of the shields, z-direction (axial) \times x-direction: 0.5×4 m in [7] and 1.2×0.52 m in our current case (Table 1).

5 Conclusions

The influence of the contact resistance on the shielding efficiency of shielding gutters for HV cables is studied with numerical simulations and experiments for two different materials: aluminium and steel. In order to observe the influence of the contact resistance on the shielding, we have performed 2D FEM, 3D FEM computations and experiments for several shielding configurations. The numerical models are validated with experimental results.

The contact resistance has been shown to have much more effect in the conductive shield than in the ferro-magnetic shield. The ratio of average induction between bad and good contact is about 1.7 with aluminium and 1.3 with steel in case of the default geometry in Table 1. The aluminium performs worse than the steel with bad contact.

Also, from the results, it was observed that bad contact has less influence if the plates have a relatively long axial length in comparison with their other dimensions. Nevertheless, the effect remains quite significant for aluminium shields with practically convenient dimensions. It should be observed that for aluminium and steel, the bad contact reduces the shielding efficiency with a factor 2 and a factor 1.17 if the axial length of a shield element is less than 3.5 times the height, respectively. The bad contact has less effect for the steel shield than aluminium shield, regardless of θ .

Parasitic air gap between the CP and the gutter has a relatively small effect on the shielding for steel, what matters is the absence of contact. Although the effect of the parasitic air gap can be seen only very close to the shield, the gap of a few millimetres does not have much effect on the shielding. Even, the size of the gap has virtually no effect on the shielding performance for aluminium.

As a result, we can say that the contact resistance between shield elements is one of the important factors affecting the performance of the shielding system and it should be taken into account in practical shielding applications.

6 Acknowledgments

The work was supported by the Scientific and Technological Research Council of Turkey (TUBITAK) and by the IAP project P6/21. P. Sergeant is a postdoctoral researcher for the 'Fund of Scientific Research Flanders' (FWO).

7 References

- 1 Hartal, O., Merzer, M., Netzer, M.: 'Shielding from ELF magnetic fields emanating from power plants in large facilities', *Environmentalist*, 2005, **25**, (2–4), pp. 209–214
- 2 Koroglu, S., Adam, A.A., Umurkan, N., Gulez, K.: 'Leakage magnetic flux density in the vicinity of induction motor during operation', *Electr. Eng. (Archiv fur Elektrotechnik)*, 2009, **91**, (1), pp. 15–21
- 3 Sergeant, P., Sabariego, R.V., Crevecoeur, G.L., Sergeant, P., Geuzaine, C.: 'Analysis of perforated magnetic shields for electric power applications', *IET Electr. Power Appl.*, 2009, **3**, (2), pp. 123–132
- 4 Sergeant, P., Dupré, L., Melkebeek, J.: 'Active and passive magnetic shielding for stray field reduction of an induction heater with axial flux', *IEE Proc. Electr. Power Appl.*, 2005, **152**, (5), pp. 1359–1364
- 5 Zucca, M., Lorusso, G., Fiorillo, F., Roccato, P.E., Annibale, M.: 'Highly efficient shielding of high-voltage underground power lines by pure iron screens', *J. Magn. Magn. Mater.*, 2008, **320**, pp. 1065–1069
- 6 Cardelli, E., Faba, A., Pirani, A.: 'Nonferromagnetic open shields at industrial frequency rate', *IEEE Trans. Magn.*, 2010, **46**, (3), pp. 889–898
- 7 Sergeant, P., Dupré, L., Melkebeek, J.: 'Magnetic shielding of buried high voltage cables by conductive metal plates', *COMPEL*, 2008, **27**, (1), pp. 170–180
- 8 De Wulf, M., Wouters, P., Sergeant, P., *et al.*: 'Electromagnetic shielding of high-voltage cables', *J. Magn. Magn. Mater.*, 2007, **316**, pp. 908–911
- 9 Dular, P., Kuo-Peng, P., Geuzaine, C., Sadowski, N., Bastos, J.P.A.: 'Dual magneto-dynamic formulations and their source fields associated with massive and stranded inductors', *IEEE Trans. Magn.*, 2000, **36**, (4), pp. 3078–3081